Corrosion effects on structural integrity and life of oil rig drill pipes

Aleksandar Sedmak[1], Radzeya Zaidi[1], Borivoje Vujičić[2], Živče Šarkočević[4], Snežana Kirin[3], Zoran Stamenić[1], Miloš Đukić[1] and Gordana Bakić[1]

[1]*University of Belgrade, Faculty of Mechanical Engineering, Serbia*
[2]*Electric Power Industry of the Republic of Srpska, Trebinje, Bosnia and Herzegovina*
[3]*Innovation center of the Faculty of Mechanical Engineering, Belgrade, Serbia*
[4]*Faculty of Technical Sciences, University of Priština with seat in Kosovska Mitrovica, Serbia*

Abstract

Corrosion effects on structural integrity and life of oil rig welded pipes are analysed by experimental, analytical, and numerical methods. Experiments were performed using standard tensile specimens and CT specimens for static loading, Charpy specimens for impact loading, and 3 Point Bending specimens for fatigue crack growth with amplitude loading. In each case new and old pipes were used to evaluate corrosion effects. Results indicated negligible corrosion effects in the case of tensile properties and impact toughness, and strong effects in the case of fracture toughness and especially fatigue crack growth rates, increasing the risk of static failure and reducing significantly structural life. Analytical expressions are used for oil rig pipe structural integrity and life assessment to quantify these effects. Recently introduced risk-based approach is applied to analyse oil rig drill pipe with a corrosion defect treated as a surface crack.

Keywords: risk-based assessment; failure analysis diagram; fatigue; risk matrix.

Available on-line at the Journal web address: http://www.ache.org.rs/HI/

ORIGINAL SCIENTIFIC PAPER

UDC: 622.24.053:67.019:539.388.1

Hem. Ind. **76(3)** 167-177 (2022)

1. INTRODUCTION

Casing steel pipes used in oil drilling rigs are subjected to a corrosive atmosphere making them susceptible to material degradation, sometimes in combination with errors in design and manufacturing. The main concern is the influence of CO_2 and H_2S in the oil and gas exploitation facilities because these gases, especially under high pressures and temperatures, create a corrosive environment [1,2]. Therefore, besides common reasons for failures of the pipelines, such as insufficient resistance to crack initiation and propagation and especially occasional inadequate quality of welded joints, corrosion defects often reduce strength and crack resistances, causing static or fatigue failure [3,4]. In this context it is necessary to analyse material resistance to cracking not only for new material, but also for material after certain period of exploitation, referred in the following text as used material. To fully comprehend the complex mechanism of corrosive action of fluids from oil and gas wells, all the factors caused by the presence of carbon dioxide, hydrogen sulfide, chloride, and mercury, affecting the initiation and development of corrosion should be taken into consideration [5,6].

Presence of flaws in the basic material or in welded joints of protective welded pipes in oil wells does not necessarily cause the loss of their integrity, [7-8]. Assessment which refers to the tolerability of some kinds of flaws depends on possible interactions of the following factors: geometry of protective welded pipes, stress states (operational and residual), type, size and location of the flaw, mechanical properties of welded joints, conditions of exploitation, *etc* [9-10]. On the basis of accurate determination of the flaw type and size and calculation of the operational ability of the welded joint, the decision regarding its use or rejection can be reached. Structural integrity is a relatively new scientific and engineering discipline, which in a broader sense comprises the state analysis and diagnostics of behaviour, lifetime evaluation and structure refurbishment. This means that, besides the common task of assessing the integrity of

Corresponding authors: Aleksandar S. Sedmak, University of Belgrade, Faculty of Mechanical Engineering, Kraljice Marije 16, 11120 Belgrade 35, Serbia; E-mail: aleksandarsedmak@gmail.com
Paper received: 25 February 2022; Paper accepted: 27 June 2022; Paper published: 18 July 2022.
https://doi.org/10.2298/HEMIND220222014S

structure when the flaw is detected using non-destructive inspection (NDI) methods, this discipline also comprises the analysis of the stress state of the structure with and without a crack.

Numerous papers have been published on pipe failures due to cracks and other defects, including corrosion, [11-16], and some of them focused on welded joints, [17]. Nevertheless, all of them lack a comprehensive approach, which would include experimental, numerical, and analytical approaches to the problem of corroded pipes and the remaining pipe strength. Toward this aim, several papers were published in the last decade by the authors of the present study, [18-22], including previous experimental investigation on the pipe taken from exploitation in an oil drilling rig after 70,000 hours (8 years) of service [23,24]. In the present paper, the new method, recently introduced and applied for pressure vessels, [25-29], is applied to assess structural integrity of API J55 steel pipes, damaged by corrosion, using risk-based approach. In respect to welded joints, focus here is on the base metal, since it was shown that it is more sensitive to cracking than the weld metal [23, 24].

2. EXPERIMENTAL METHODS

API J55 steel, with the chemical composition shown in Table 1, and metallographic examination shown in Figure 1, indicating typical rolled ferrite-pearlite microstructure, is used here for testing as a common material for oil rig drilling pipes. Specimens were cut from the casing pipe manufactured by high frequency (HF) welding - producer US Steel, Serbia). The pipe was withdrawn from a drilling rig during a reparation procedure after about 70000 hours (8 years) of operation. At the same time, new pipe was used for testing both the material properties and pipe behaviour under pressure [23]. Testing of tensile properties, impact toughness, fracture toughness and fatigue crack growth rate is presented in the following text. Specimens were cut out from both new and used pipes and machined to standard dimensions for each testing.

Table 1. Chemical composition of API J55 steel [23]

Element	C	Si	Mn	P	S	Cr	Ni	Mo	V	Cu	Al
Content, wt.%	0.29	0.23	0.96	0.013	0.022	0.1	0.058	0.012	0.003	0.13	0.025

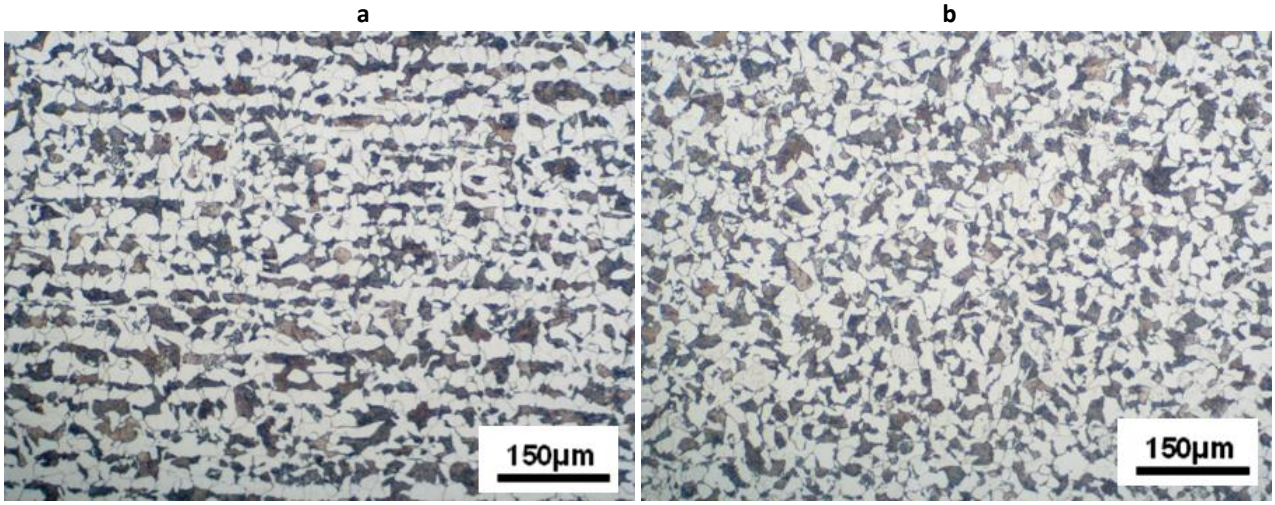

Fig. 1. Microstructure of API J55 steel: a) rolling direction; b) transverse direction [23]

2. 1. Tensile properties

Tensile properties were tested in accordance with the standard ASTM E8-08, [30], using specimens of the base metal prepared according to the standard ASTM A370, Fig. 2, [31], as shown in [21,23]. Testing was done by using the electromechanical testing machine, SCHENCK-TREBEL RM 100 (SCHENCK - Germany), in displacement control, with the rate 5 mm/min.

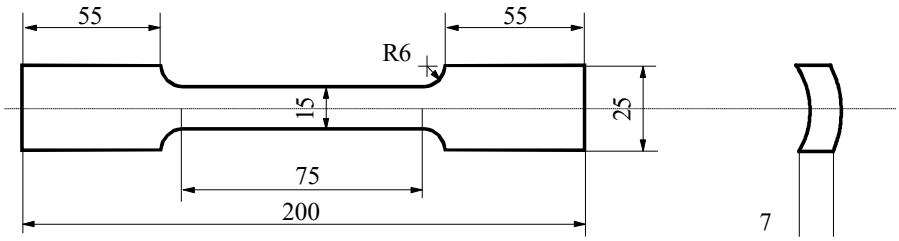

Fig. 2. Specimens for tensile testing [23]

2. 2. Impact toughness

Impact toughness was tested by using the instrumented Charpy pendulum SCHENCK TREBELL 150/300 and Charpy specimens, Fig. 3, according to the standard ASTM E23-01 [32], as shown in more details in [23]. Instrumented pendulum enables separation of energies for crack initiation and propagation, which are equally important indicators of material behaviour under impact loading, as the total energy.

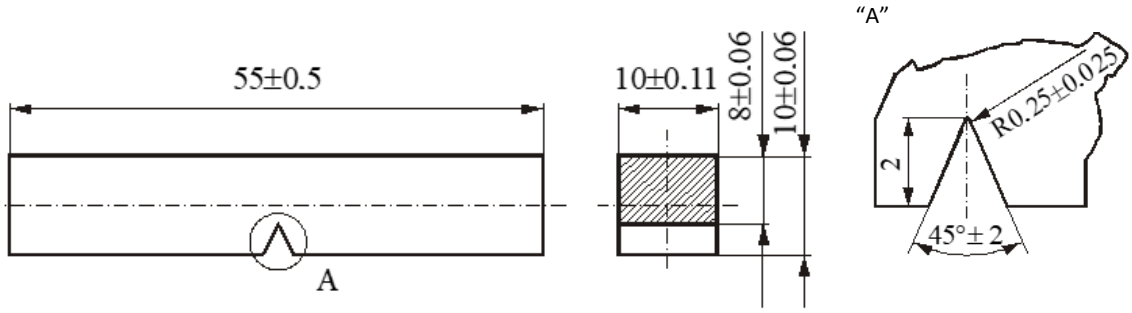

Figure 3. Charpy specimen for impact toughness testing

2. 3. Fracture toughness

Keeping in mind that the material tested here is not a brittle one, it was necessary to use elastic-plastic fracture mechanics parameter, such as *J* integral, to estimate fracture toughness [33]. Toward this aim, so-called crack resistance curves, *i.e. J-R* curves, are used to get the critical J_{Ic} value, which is then used to calculate K_{Ic}, *i.e*. the fracture toughness, according to the standard ASTM E1820, [33]. To obtain *J-R* curves and J_{Ic} values, relevant for real pipes, standard compact tension (CT) specimens were used and modified, since they were directly cut out from new and used pipes, with curvature and thickness as shown in Fig. 4, [14,19,23]. Testing was done by using the electromechanical testing machine, SCHENCK-TREBEL RM 100, using special grips for CT specimens.

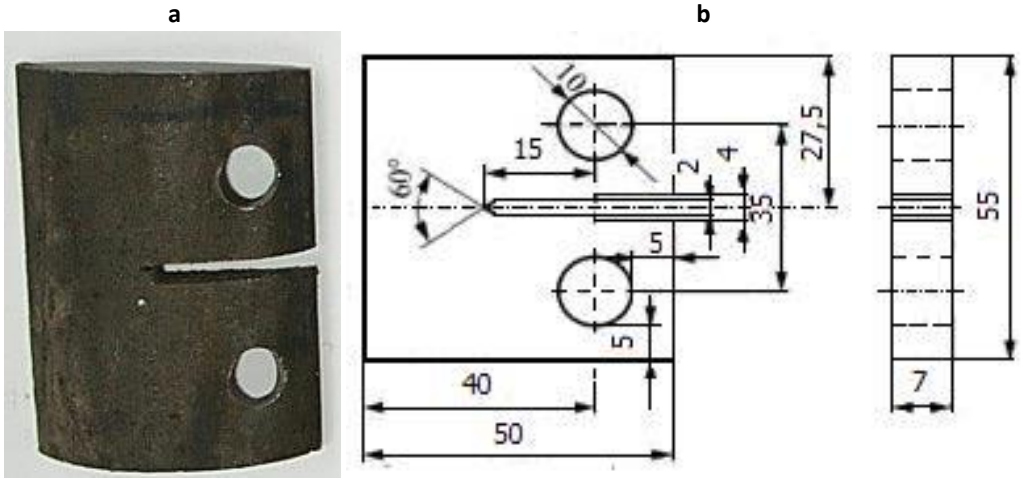

Figure 4. CT specimen: a) photograph, b) dimensions

2. 4. Fatigue Crack Growth testing

Fatigue crack growth (FCG) was tested at room temperature, in accordance with ASTM E647, [34] using Three Point Bending (3PB) specimen on a Fractomat device (Rumul, Switzerland), as shown in Fig. 5, and explained in more details in [23].

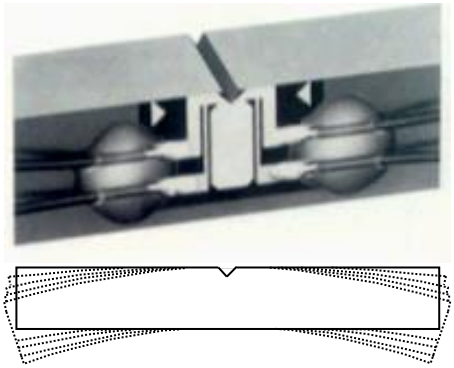

Fig. 5. Fatigue crack growth testing: 3PB specimen with foil for measuring the crack length assembly

2. 5. Prototype testing

Testing of prototype was conducted on a pressure vessel with defects of the circular shape. The vessel was made from a part of the casing pipe made by HF welding of API J55 steel, closed at both ends with nominal dimensions: diameter ϕ139.7 mm, wall thickness 6.98 mm, Fig. 6a. In the experiment performed [23], strain gages and rosettes were used to evaluate *J* integral by so-called the direct measurement technique. Different artificially made surface defects with lengths D = 26, 28, and 30 mm and depths a = 1.75, 3.5, and 5.25 mm (Fig. 6b) were monitored to assess their effects on structural integrity [21,23].

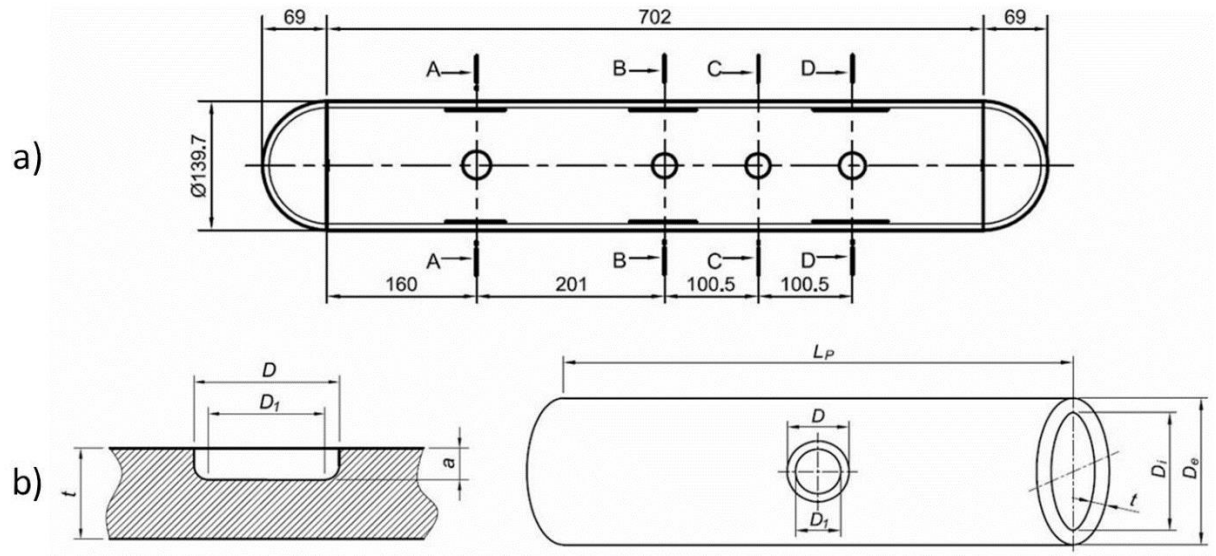

Fig. 6. a) Prototype with artificial defects, b) defect details

3. RESULTS

3. 1. Tensile testing

Results of tensile testing are shown in Table 2 for the new and used material, respectively. As one can see, yield stress (R_e) is significantly reduced due to damage in used material, while tensile strength (R_m) and elongation (A_5) are not significantly affected. One possible explanation of such a behaviour could be that damage has reversed the

mechanism used to obtain unusually high R_e of the new material, but this phenomenon is yet to be investigated. Anyhow, it is considered here as a fact indicating the corrosion effect on tensile properties. It should be also noticed that the hardness values were almost the same, 195±10 in both cases [23].

Table 2. Tensile properties for new and used material [23]

R_e ± SD / MPa		R_m ± SD / MPa		A_5 ± SD / %	
New material	Used material	New material	Used material	New material	Used material
547.7±7.6	379.7±3.3	586.7±6.2	562.3±2.9	28.7±1.3	33.0±1.2

3. 2. Impact toughness

Impact toughness values determined for the new and used material are shown for different testing temperatures in Table 3, indicating weak influence of corrosion damage. All other details and results are shown in [30], including the effect of different microstructures in the base metal (BM), weld metal (WM) and heat-affected-zone (HAZ), which turned out to be insignificant.

Table 3. Impact toughness for new / used material

Mean value ± standard deviation

Testing temperature, °C	E_{uk} ± SD / J	
	New material	Used material
–40	26.3±3.1	26.7±3.7
–20	52.3±0.9	54.3±2.5
+20	99.0±0.0	102.3±6.1

3. 3. Fracture toughness

Fracture toughness values are shown in Table 4, indicating stronger influence of corrosion damage than in the case of tensile properties and impact toughness. Of special interest are minimum K_{Ic} values, 121.4 MPa·m$^{0.5}$ for the new material, and 91.4 MPa·m$^{0.5}$ for the used one, in both cases for the base metal, as the most sensitive to cracking.

Table 4. Fracture toughness K_{Ic}, new / used material

Crack location	K_{Ic} / MPa·m$^{0.5}$	
	New material	Used material
Base metal	121.4	91.4

3. 4. Fatigue crack growth testing

Results for the threshold values, ΔK_{th}, and Paris law coefficients C and m, are shown in Table 5 for new and used material, tested with amplitude loading corresponding to the stress intensity factor range ΔK=15 MPa·m$^{0.5}$. More detailed results, including relation between the FCG rate, da/dN, and stress intensity factor range, ΔK, are presented in form of a diagram in [14,23]. Here, the FCG rate is presented for the stress intensity factor range ΔK=15 MPa·m$^{0.5}$, indicating a strong effect of corrosion damage, since the FCG rate is almost 6-fold higher for the used material.

Table 5. Fatigue crack growth parameters, [23]

	ΔK_{th} / MPa·m$^{0.5}$	C	m	(da/dN) / (m / cyc) (ΔK=15 MPa·m$^{0.5}$)
New material	9.5	$1.23\cdot10^{-13}$	3.931	$5.17\cdot10^{-9}$
Used material	9.2	$2.11\cdot10^{-15}$	6.166	$3.75\cdot10^{-8}$

To summarize, there is insignificant influence of corrosion on tensile properties and impact toughness, but both fracture toughness and especially FCG rate are strongly affected, indicating potential large differences in structural integrity and life assessment.

3. 5. Prototype testing

Experimental results of prototype testing are shown in Figure 7 in the form of *J* integral *vs*. pressure, and explained in more details in [20], including comparison with FEM, indicating safe operation at the design pressure of 10 MPa. One can note that failure did not occur for testing pressure as high as 22 MPa.

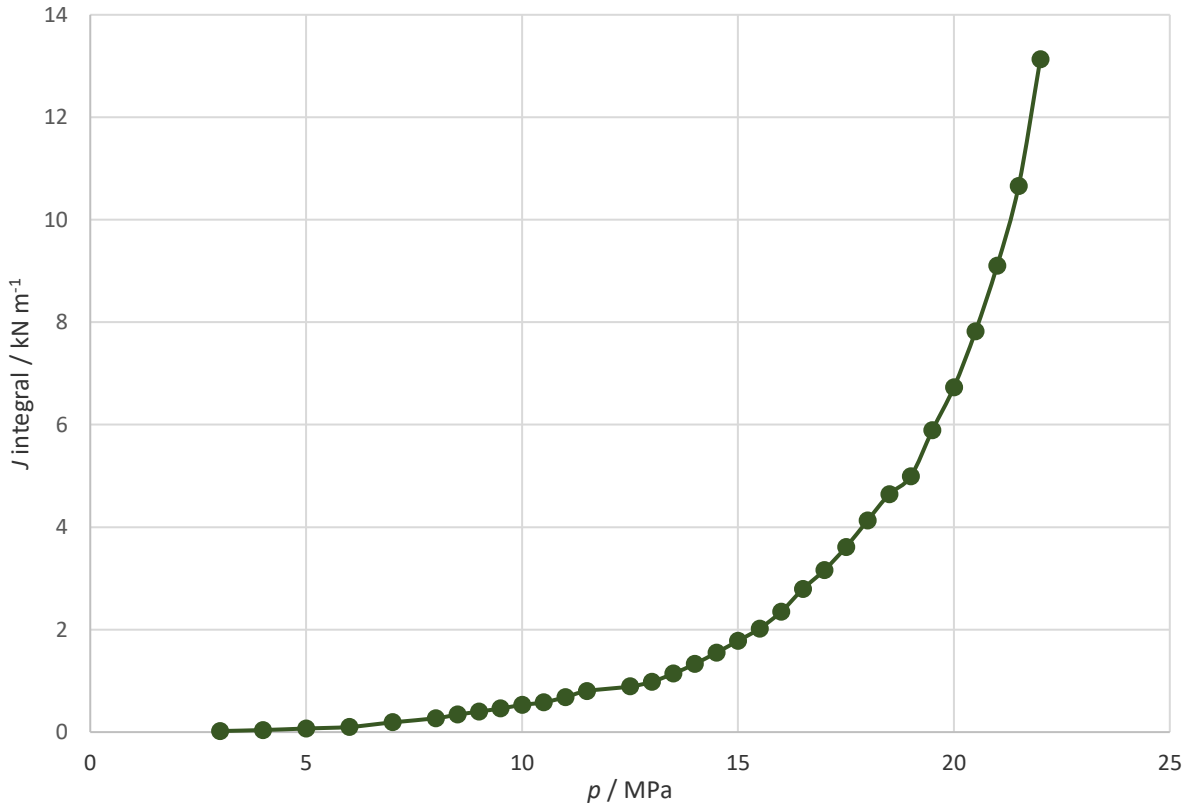

Figure 7. Prototype testing results - J integral vs. pressure

4. STRUCTURAL INTEGRITY ASSESSMENT

Analytical assessment of structural integrity is based on calculation of the stress intensity factor and stress ratio, with an aim to define the corresponding point in the Failure Analysis Diagram (FAD) [35]. Basic concept of the FAD, shown in Figure 8, is that a point below the limit line is safe, while a point outside the limit line is not safe. The limit line is defined by equation (1):

$$K_r = S_r \left[\frac{8}{\pi^2} \ln \sec \left(\frac{\pi}{2} \cdot S_r \right) \right]^{0.5} \quad (1)$$

where K_r is the ratio between the stress intensity factor K_I and its critical value K_{Ic}, while S_r is the ratio between the net stress S_{net} and the stress critical value S_c.

To evaluate points in the case analysed here, the stress intensity factor K_I is calculated according to the following equation (2):

$$K_I = YS\sqrt{\pi a} \quad (2)$$

where Y is the geometry factor, depending on the crack type and size, [24], $S = p \cdot r/t$ is the circumferential stress in a thin cylindrical vessel, p is the pressure, r radius, and t thickness. The net stress is calculated in the same way as S, but for the reduced cross-section, where the crack is located.

The critical value of K_I, *i.e*. fracture toughness K_{Ic}, is already defined in Table 4, whereas the critical value of stress, S_c, is commonly defined as the mid-value of yield and tensile strengths, equation (3)[23]:

$$S_C = \frac{R_e + R_m}{2} \tag{3}$$

For calculation of the above parameters a crack with the depth a = 3.5 mm and length $2c$ = 28 mm was considered. The cross section reduction is then (3.5×28)/(6.98×702)=0.0200, and net stress S_{net}=100/0.9800=102.0 MPa. According to the data given in Table 2, the critical stress is S_c= (547.7+586.7)/2=567.2 MPa for the new material, and S_c=(379.7+562.3)/2=471 MPa for the used one. Now, one can calculate the X coordinate as by equation (4):

$$X = \frac{S_{net}}{S_c} \tag{4}$$

These values are 0.19 and 0.23 for the new and used material at the pressure of 10 MPa, respectively. Corresponding values for the pressure of 22 MPa are 0.42 and 0.51, respectively.

To get the Y coordinate, the stress intensity factor for a surface edge crack in a cylinder is needed. It can be obtained by using different methods for geometry factors, depending on the crack size [36]. According to the procedure explained in [24], the geometry factor for the crack 3.5 mm in depth and 28 mm in length is Y_{total}=2.538, and the corresponding stress intensity factor is K_I=32.6 MPa·m$^{0.5}$ for the pressure of 10 MPa and 71.7 MPa·m$^{0.5}$ for the pressure of 22 MPa. Taking into account the critical values of stress intensity factor from Table 4 (K_{Ic}=91.4 MPa·m$^{0.5}$ for the used material, and 121.4 MPa·m$^{0.5}$ for the new one), the Y coordinate becomes 0.35 for the used material and 0.27 for the new one (pressure 10 MPa), and 0.77 for the used material and 0.59 for the new one (pressure 22 MPa). All four points are in the safe region, as shown in Figure 8, indicating also good agreement with the experimental results.

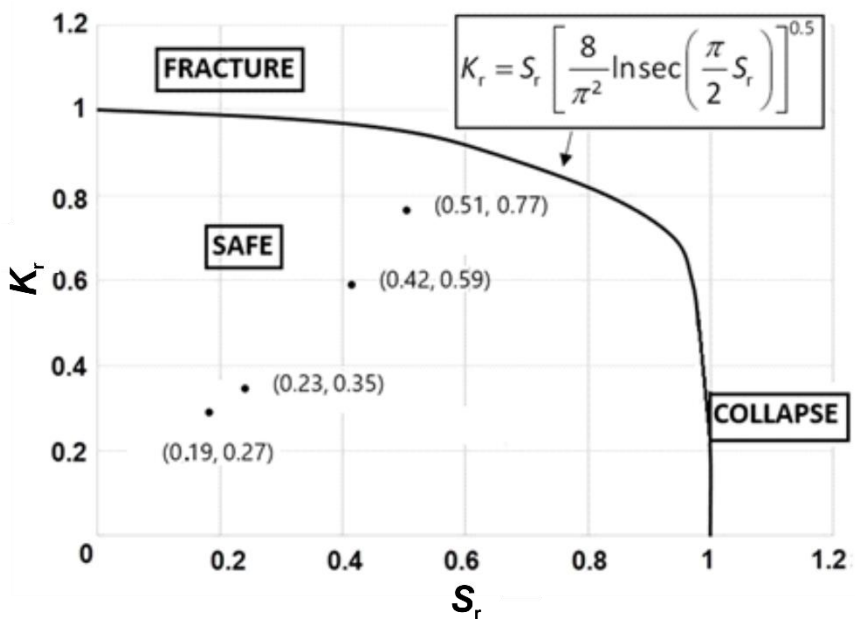

Fig. 8. Failure analysis diagram: pressure 10 MPa: new (0.19, 0.27) and used (0.23, 0.35) material; pressure 22 MPa: new (0.42, 0.59) and used material (0.51, 0.77)

Probability of failure can be now estimated according to the position of these 4 points. Using the novel procedure, one obtains 0.28 and 0.37 for the pressure of 10 MPa, new and used material, respectively, as well as 0.62 and 0.82 for the pressure of 22 MPa, also for the new and used material, respectively. Having in mind the medium consequence, as explained in [22], one obtains the risk matrix, Table 6, indicating high risk level for the pressure of 22 MPa and used material.

This is the crucial point in the analysis performed here. One should notice that the risk-based analysis shows in a simple way that material aging increases the risk for one category, whereas testing over-pressure does it for two categories! Obviously, material aging cannot be avoided, but over-pressure has to be reduced as much as possible. According to this analysis, 30 % should be the maximum value to keep all points at the medium risk level.

Table 6. Position of assessment points in the risk matrix

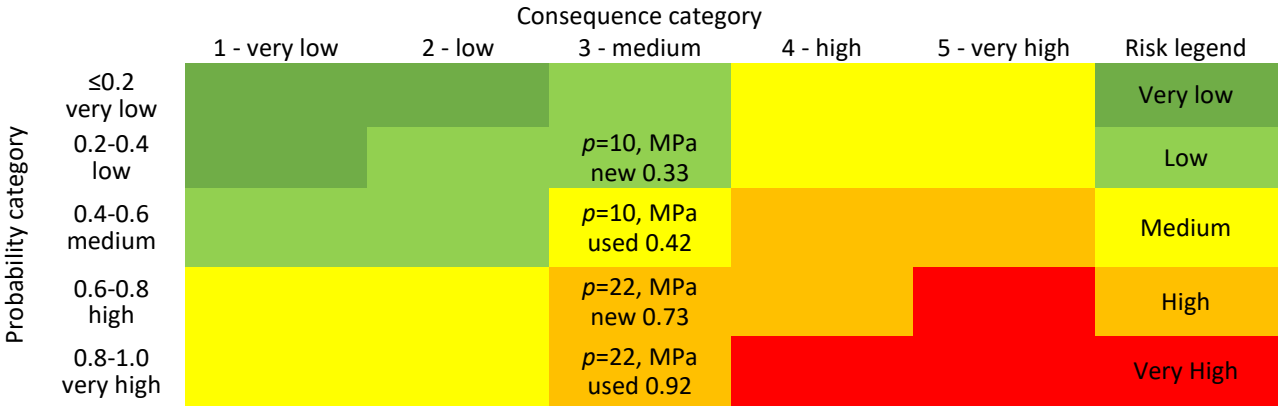

3. 3. Structural life assessment

According to the results of FCG rates, presented in Table 5, one should expect significant reduction of fatigue life of corrosion damaged material. To evaluate this detrimental effect, the Paris law was used for both analytical and numerical calculations in the following equation, as shown in equation (5) [24]:

$$\frac{\mathrm{d}a}{\mathrm{d}N} = C\left(\Delta K\right)^m = C\left(Y\left(\frac{a}{W}\right)\Delta\sigma\sqrt{\pi a}\right)^m \tag{5}$$

where $Y(a/W)$ is the geometry factor depending on the crack geometry. The Paris law can be integrated directly if one neglects dependency of the geometry parameter Y on crack geometry, or numerically if dependency is taken into account, as was done here by dividing the range of crack depth growth as follows: 3.5; 4.19; 4.88; 5.57; 6.26; 6.9; 7 mm. Coefficients C and m are used for the new and used BM, as given in Table 5. The geometry coefficient $Y(a/W)$ was in the range from 2.39 to 4.29, also affected by different crack lengths. Amplitude loading is defined as R=0.79 (in ABAQUS input data file) for 21 MPa (maximum stress 100 MPa, minimum stress 79 MPa, [23]). Calculation is based on the *Raju-Newman* solution for a surface crack in a thin-walled cylindrical shell, equation (6)[36]:

$$K_{\mathrm{I}} = \left[M_{\mathrm{f}} + \left(E_{\mathrm{k}}\sqrt{\frac{c}{a}} - M_{\mathrm{T}}\right)\left(\frac{a}{t}\right)^s\right]\frac{\sigma\sqrt{\pi\cdot a}}{E_{\mathrm{k}}}\cdot M_{\mathrm{tm}} \tag{6}$$

where: M_{f} is a function depending on the crack geometry (on the ratio a/c); s is the function depending on the crack geometry (on the ratio a/c) and on the relative crack depth (on the ratio a/t); $_{\mathrm{tm}}$ (M_s) is the surface correction factor for a surface crack and M_{T} is the Folias correction factor.

To fit the Raju and Newman results for the deepest point $\theta = \pi/2$, the parameter (s) is given by equation (7):

$$s = 1.6 + 3\left(a/c\right)^3 + 8\left(a/c\right)\left(a/t\right)^5 + 0.008\left(a/c\right) \tag{7}$$

Results obtained in this way are presented in Table 7. The presented data indicate cca 17 % reduction of fatigue life for the used material as compared to the new one.

Table 7. Data for crack length 2C = 28 mm, using parameters M_f, E_k, S, M_T, M_{Tm} and F_{total} as defined in [24]

a / mm	c/a	a/t	a/c	M_{f}	E_{k}	S ($\theta = \pi/2$)	M_{T}	M_{Tm}	Y_{total}	K_1 / MPa·m$^{0.5}$	a_c / m		N ($\theta = \pi/2$)	
											old	new	old	new
3.5	4.000	0.501	0.250	1.105	1.149	1.742	1.022	1.016	2.448	25.69	0.200	0.353	0	0
4.19	3.341	0.600	0.299	1.100	1.200	1.894	1.032	1.032	2.483	28.51	0.191	0.337	7029810	6254403
4.88	2.869	0.699	0.349	1.095	1.257	2.216	1.043	1.060	2.557	31.69	0.173	0.305	10536232	10520849
5.57	2.513	0.798	0.398	1.090	1.320	2.839	1.055	1.110	2.716	35.96	0.145	0.255	12092670	13392910
6.26	2.236	0.897	0.447	1.085	1.388	3.962	1.069	1.207	3.074	43.14	0.108	0.190	12586914	15166127
6.9	2.029	0.989	0.493	1.081	1.456	5.697	1.083	1.405	3.910	57.60	0.069	0.121	12661710	15985600
7	2.000	1.003	0.500	1.080	1.466	6.049	1.086	1.456	4.144	61.50	0.062	0.110	12668570	16030191

4. DISCUSSION

In order to verify the approach applied in this research, results are now compared with the experimental and numerical ones, presented in [21]. To do so, the maximum allowed pressure has been calculated according to the critical value taken from the failure analysis diagram (FAD) for the used material, leading to p=26.8 MPa (22/0.82), since the probability level for the pressure 22 MPa is 0.82, and for the allowed (critical) pressure it is 1. Maximum allowed pressures, as given in [21] for 3 analytical and FEM values obtained for 3 different reference stresses (0.8, 0.85, and 0.9 of the ultimate tensile strength - UTS), are in the range 37.1 to 48.2 MPa. The maximum allowed pressure calculated based on FAD is clearly lower than any of them. Taking into account the fact that these values are obtained for the real geometry of defect, it is easy to conclude that the significantly smaller value obtained here is in accordance with the fact that the defect is considered as a surface crack, whereas in analytical and numerical calculations it was treated as a geometry imperfection. In this way, our approach is verified as a conservative and reliable, and also as a simple one.

Results for remaining life, *i.e* the number of cycles needed for crack growth from the initial depth (3.5 mm) to 6.26 mm, for crack length 28 mm, Table 7, are also given in Table 8 for the used and new material to show more clearly the effect of material aging. One can see that this effect is important, but not significant, since the reduction in the remaining life is 17 %, from about 2.8 years for the new material to about 2.3 years for the used material. One can notice that the effect is much more pronounced for a longer crack, as presented [22], and also shown here in Table 8.

Table 8. Number of cycles N and remaining life for crack growth in depth from 3.5 to 6.26 mm

Crack length	*N*		Time, year*	
	Used material	New material	Used material	New material
2*c*=28 mm	12,586,914	15,166,127	2.328	2.805
2*c*=200 mm **	464,212	2,433,641	0.092	0.482

*1 year=5,046,009 cycles, **data taken from [22]

One issue remains critical in the approach presented here. Namely, as shown in [24], analytical expressions do not exist for evaluation of surface crack stress intensity factors, which would be the best approach for crack analysis regardless the crack type and size. In this research, the Raju-Newman expression is used, but its validity for very deep cracks is questionable. Anyhow, analytical expressions used here are useful and present a practical engineering tool to assess structural integrity and life of a cracked corroded component in a simple way.

5. CONCLUSIONS

According to the presented analysis of oil rig welded pipes, following conclusions can be drawn.

- Fracture toughness and FCG rate are strongly affected by corrosion damage, although tensile properties and impact toughness are not. This is probably valid for ferritic steels in general, but not austenitic ones.
- The most pronounced effect of corrosion damage is in the case of amplitude loading, since it increases the FCG rate up to 6 times, which in turn significantly reduces structural life. Anyhow, this result should not be generalized, since it is specific for the case studied here.
- Corrosion damage increases the failure risk for one category (low to medium - working pressure, high to very high – test pressure), whereas the increase from working to testing pressure increases the failure risk for two categories (from low to high – new material, medium to very high – used material).
- Testing pressure has to be reduced as much as possible. According to this analysis, 30 % should be the maximum value to keep the risk at medium level. The optimal value should be 10 %.
- Failures due to relatively short cracks can be prevented by timely intervention, what might not be the case for relatively long cracks.

Acknowledgement: This research was supported by the Ministry of Education, Science and Technological Development of the Republic of Serbia (contracts 451-03-9/2021-14/200105 and 451-03-9/2021 -14/200213).

REFERENCES

[1] Popoola LT, Grema AS, Latinwo GK, Gutti B, Balogun AS. Corrosion problems during oil and gas production and its mitigation, *Int J Ind Chem.* 2013; 4(1); 35; http://dx.doi.org/10.1186/2228-5547-4-35

[2] Wasim M, Djukic M. External corrosion of oil and gas pipelines: A review of failure mechanisms, *J Nat Gas Sci Eng*. 2022; 100: 104467, https://doi.org/10.1016/j.jngse.2022.104467

[3] Perez TE. Corrosion in the oil and gas industry: an increasing challenge for materials, *JOM* 2013; 65(8): 1033-1042; https://doi.org/10.1007/s11837-013-0812-z

[4] Sharma SK, Maheshwari S. A review on welding of high strength oil and gas pipeline steels. *J Nat Gas Sci Eng* 2017; 38: 203-217; ISSN: 1875-5100

[5] Askari M, Aliofkhazraei M, Afroukhteh, S. A comprehensive review on internal corrosion and cracking of oil and gas pipelines, *J Nat Gas Sci Eng.* 2019; 71: 102971; https://doi.org/10.1016/j.jngse.2019.102971

[6] http://earth.uni-muenster.de/earth/d/dokumente/schlumberger/English/Corrosion/, 05.1999

[7] Šarkoćević Ž, Arsić M, Medjo B, Kozak D, Rakin M, Burzić Z, Sedmak A. Damage level estimate of API J55 steel for welded seam casing pipes. *Strojarstvo: J Theory Appl Mech Eng* 2009; 51: 303-311; https://doi.org/10.1016/j.mspro.2014.06.155

[8] Lazić Vulićević Lj, Arsić M, Šarkoćević Ž, Sedmak A, Rakin M. Structural life assessment of oil rig pipes made of API J55 steel by high frequency welding, *Technical gazette* 2013; 20(6): 1091-1094; ISSN: 1330-3651

[9] Medjo B, Rakin M, Gubeljak N, Matvienko Y, Arsic M, Sarkocevic Z, Sedmak A. Failure resistance of drilling rig casing pipes with an axial crack, *Eng Fail Anal*. 2015; 58: 429-440; https://doi.org/10.1016/j.engfailanal.2015.05.015

[10] Rakin M, Medjo B, Arsić M, Šarkoćević Z, Sedmak A. Effect of exploitation conditions and flaw geometry on the load carrying capacity of casing pipes for oil drilling rigs, *Key Eng Mat.* 2012; 488-489: 577-580; https://doi.org/10.1016/j.mspro.2014.06.155

[11] Azevedo CRF, Sinatora A. Failure analysis of a gas pipelines, Instituto de Pesquisas Tecnologicas do Estado de Sao Paulo, *Eng Fail Anal*. 2004; 11: 387-400; https://doi.org/10.1016/j.engfailanal.2003.06.004

[12] Assanelli AP, Toscano RG, Johnson DH, Dvorkin EN. Experimental/numerical analysis of the collapse behavior of steel pipes. *Eng Computat.* 2000; 17: 459 - 86.

[13] Fu B, Batte AD. Advanced Methods for the Assessment of Corrosion in Linepipe, Health and Safety Executive Summary Report, OTO 1999-051, HSE Books, 1999; https://www.hse.gov.uk/research/otopdf/1999/oto99051.pdf

[14] Kiefner J, Vieth PA. Modified criterion for evaluating the strength of corroded pipe, Final Report for PR 3-805 project to the Pipeline Supervisory Committee of the American Gas Association, Battelle, Ohio, 1989.; https://www.worldcat.org/title/final-report-on-project-pr-3-805-a-modified-criterion-for-evaluating-the-remaining-strength-of-corroded-pipe/oclc/43015134

[15] Kiefner J, Vieth P. Evaluating pipe - 1 new method corrects criterion for evaluating corroded pipe, *Oil & Gas J*. 1990; 6: 56-9

[16] Fu B, Kirkwood M. Predicting failure pressure of internally corroded linepipe using the finite element method, OMAE95, *Pipeline Technology*, international conference on offshore mechanics & arctic engineering, 1995; V: 175-85.; ISBN 0-7918-1311-8; TRN: IM9615%%245

[17] Lee J-S, Ju J-B, Jang J, Kim W-S, Kwon D. Weld crack assessments in API X65 pipeline: failure assessment diagrams with variations in representative mechanical properties, *Mat Sci Eng.* 2004; 373: 122-30; https://doi.org/10.1016/j.msea.2003.12.039

[18] Rakin M, Medjo B, Arsić M, Šarkoćevic Ž, Ivanović I, Sedmak A. API J55 steel casing pipe with an initial surface crack under internal pressure - Determination of fracture parameters, *Key Eng Mat.* 2014; 601: 65-70; 10.4028/www.scientific.net/KEM.488-489.577

[19] Rakin M, Arsić M, Medjo B, Šarkoćević Ž, Sedmak A. Structural integrity assurance of casing pipes in the oil and gas industry, *WIT Trans Built Environ.* 2013; 134: 401-410; https://doi.org/10.2495/SAFE130361

[20] Kirin S, Sedmak A, Zaidi R, Grbović A, Šarkočević Ž, Comparison of experimental, numerical and analytical risk assessment of oil drilling rig welded pipe based on fracture mechanics parameters, *Eng Fail Anal*. 2020; 114(4); https://doi.org/10.1016/j.engfailanal.2020.104600

[21] Sedmak A, Arsić M, Šarkoćević Ž, Medjo B, Rakin M, Arsić D, Lazić M. Remaining strength of API J55 steel casing pipes damaged by corrosion, *Int J Press Vess Piping*. 2020; 188; https://doi.org/10.1016/j.ijpvp.2020.104230

[22] Zaidi R, Kozak D, Sedmak A, Kirin S, Franulovic M. Risk assessment based on analytical evaluation of structural integrity and life of drilling rig pipe, *Procedia Struct. Integr.* 2021; 33: 1181-1186; https://doi.org/10.1016/j.prostr.2021.10.132

[23] Šarkoćević Ž. Resistance to Damage and Fracture of Protective Welded Pipes in Oil Wells, Ph.D. Dissertation (in Serbian), University of Belgrade, 2010.

[24] Zaidi R. Application of fracture mechanics parameters to residual life assessment of welded pipes exploitation under fatigue loading, Ph.D. Dissertation, University of Belgrade, 2021.

[25] Golubović T, Sedmak A, Spasojević Brkić V, Kirin S, Rakonjac I. Novel risk based assessment of pressure vessels integrity. *Technical Gazette* 2018; 25: 803-807; https://doi.org/10.17559/tv-20170829144636

[26] Zaidi R, Sedmak A, Kirin S, Martić I, Šarkočević Z. Structural integrity and life assessment of oil drilling rig pipes using analytical method, *Struct Integ Life*. 2022; 22: 63-68

[27] Sedmak A, Algool M, Kirin S, Rakicevic B, Bakic R. Industrial safety of pressure vessels - Structural integrity point of view, *Hem. Ind* 2016; 70: 685-694; https://doi.org/10.2298/HEMIND150423005S
[28] Golubović T, Sedmak A, Spasojević Brkić V, Kirin S, Veg E. Welded joints as critical regions in pressure vessels – case study of vinyl-chloride monomer storage tank, *Hem Ind.* 2018; 72(4): 177-182; https://doi.org/10.2298/HEMIND171009006G
[29] Zaidi R, Sedmak A, Kirin S, Grbovic A, Li W, Lazic Vulicevic L, Sarkocevic Z. Risk assessment of oil drilling rig welded pipe based on structural integrity and life estimation, *Eng. Fail Analysis*. 2020; 112: 104508; https://doi.org/10.1016/j.engfailanal.2020.104508
[30] ASTM E8/E8M-08, Standard Test Methods for Tension Testing of Metallic Materials
[31] ASTM A370-20, Standard Test Methods and Definitions for Mechanical Testing of Steel Products
[32] ASTM E23-01, Standard Test Methods for Notched Bar Impact Testing of Metallic Materials
[33] ASTM E1820-20, Standard Test Method for Measurement of Fracture Toughness
[34] ASTM E647 - 15e1 Standard Test Method for Measurement of Fatigue Crack Growth Rates
[35] BS 7910:2005 Guide to methods for assessing the acceptability of flaws in metallic structures, vol. 3, 2005
[36] FITNET Fitness-for-service (FFS) Annex, (2008), Volume 2, ISBN 978-3-940923-01-1

Efekti korozije na integritet konstrukcije i životni vek cevi za bušenje izvora nafte

Aleksandar Sedmak[1], Radzeya Zaidi[1], Borivoje Vujičić[2], Živče Šarkočević[4], Snežana Kirin[3], Zoran Stamenić[1], Miloš Đukić[1] i Gordana Bakić[1]

[1]Univerzitet u Beogradu, Mašinski fakultet, Beograd, Srbija
[2]Direkcija za proizvodnju električne energije, Trebinje, Bosna i Hercegovina
[3]Inovacioni centar Mašinskog fakulteta, Beograd, Srbija
[4]Fakultet tehničkih nauka, Univzitet u Prištini sa sediptem u Kosovskoj Mitrovici, Srbija

(Naučni rad)

Izvod

Uticaj korozije na integritet i vek naftnih bušećih cevi je analiziran eksperimentalnim, analitičkim i numeričkim metodama. Eksperimenti su rađeni na standardnim zateznim i "CT" epruvetama, ispitinim statičkim opterećenjem, Šarpi epruvetama ispitanim na udarno opterećenje i epruvtama na savijanje u 3 tačke, ispitanim na amplitudno opterećenje. U svakom slučaju je ispitan novi i korišćeni materijala da bi se odredio uticaj korozije. Rezultati su ukazali na mali uticaj korozije u slučaju zateznih svojstava i žilavosti, a relativno veliku uticaj u slučaju žilavosti loma I brzine rasta zamorne prsline, što značajno povećava rizik od loma i smanjuje preostali vek cevi. Kvantifikacija ovog uticaja je određena pomoću analitičkih izraza za factor integriteta napona. Nedavno uvedeni pristup analizi rizika je primenjen da se odredio nivo rizika u novim i korićenim cevima, pri proračunskom i ispitnom pritisku.

Ključne reči: procena rizika; dijagram analize loma; zamor; matrica rizika